

An Unusual Reaction of Bis(dimethylglyoximato) Complexes: Synthesis and Characterization of Rhodium(III) Complexes Containing an Oxime–Imine Equatorial Moiety

R. Dreos,^{*,†} G. Tazzer,[†] S. Geremia,[‡] L. Randaccio,[†] F. Asaro,[†] G. Pellizer,[†]
C. Tavagnacco,[†] and G. Costa[†]

Dipartimento di Scienze Chimiche, Università di Trieste, Via L. Giorgieri 1, 34127 Trieste, Italy,
and Dipartimento di Scienze dei Materiali e della Terra, Università di Ancona,
Via Brece Bianche, I-60131 Ancona, Italy

Received November 5, 1993[⊗]

Upon reaction of $\text{Rh}^{\text{I}}(\text{Hdmg})_2$ (Hdmg = dimethylglyoximato monoanion) with phosphines of small cone angle, such as PEt_3 , PBU^n_3 , and PPh_2Me , an oxime group of one of the two equatorial dimethylglyoximato ligands is converted into an imine group. The reaction product is the $[\text{Rh}^{\text{III}}(\text{Hdmg})(\text{Hbdio})(\text{PR}_3)_2]^+$ complex, where the ligands Hdmg and Hbdio (Hbdio = 2,3-butanedione 2-imine 3-oximato) are bound to Rh(III) through four nonequivalent nitrogen atoms and the two phosphines are in trans positions. The asymmetry of the equatorial moiety is also reflected in the inequivalence of the phosphine phenyls in the NMR spectra of $[\text{Rh}(\text{Hdmg})(\text{Hbdio})(\text{PPh}_2\text{Me})_2]^+$. The complex $[\text{Rh}(\text{Hdmg})(\text{Hbdio})(\text{PEt}_3)_2]^+ [\text{Rh}(\text{Hdmg})_2(\text{Cl})_2]^- \cdot \text{H}_2\text{O}$ crystallizes in the space group $P\bar{1}$ with cell parameters $a = 8.181(3) \text{ \AA}$, $b = 11.245(4) \text{ \AA}$, $c = 11.579(5) \text{ \AA}$, $\alpha = 92.16(2)^\circ$, $\beta = 94.47(2)^\circ$, $\gamma = 98.67(2)^\circ$. The structure was refined to final $R = 0.033$ using 4690 independent reflections. The solution of the structure revealed that the crystal is built up by anions $[\text{Rh}(\text{Hdmg})_2(\text{Cl})_2]^-$, disordered cations $[\text{Rh}(\text{Hdmg})(\text{Hbdio})(\text{PEt}_3)_2]^+$, and water molecules of crystallization in the ratio 1:1:1. The cation binds one H_2O molecule through two hydrogen bonds involving the adjacent oxime O and imine N atoms. Polarographic and CV studies show that the product of the mono-electronic reduction of $[\text{Rh}(\text{Hdmg})(\text{Hbdio})(\text{PEt}_3)_2]^+$ loses a phosphine and the Rh(I) species obtained by further reduction reacts with the Rh(III) starting compound to give a Rh(II) species.

Introduction

Despite the interest in rhodium complexes as catalysts or catalyst precursors, the coordination chemistry of this metal in its bis(dimethylglyoximato) complexes (rhodoximes, Figure 1a) is by far less understood than that of bis(dimethylglyoximato)-cobalt complexes (cobaloximes).

Both in the rhodoximes and in the cobaloximes the equatorial moieties do not usually undergo reaction except for the acid–base equilibria involving the hydrogen bonds.¹ Modifications of the equatorial ligands have been observed in organocobaloximes as a consequence of the cleavage of the cobalt–carbon bond and the migration of the alkyl group.² Some uncertainties still persist about the site of the migration. Gaudemer et al. suggested that the intermediates formed in electrochemical reductions of the organocobaloximes bear the alkyl group on the nitrogen atom of the oxime group,³ in analogy with the metal to ligand *N*-alkyl migrations observed in a great number of metalloporphyrins.⁴ Recently it was proved that in the photolysis of the complex $\text{Co}[\text{C}_2(\text{DO})(\text{DOH})\text{pn}](\text{C}_6\text{H}_5\text{CH}_2)\text{I}$ the benzyl group migrates to the carbon atom adjacent to the oxime nitrogen.⁵ The cleavage of the cobalt–carbon bond can

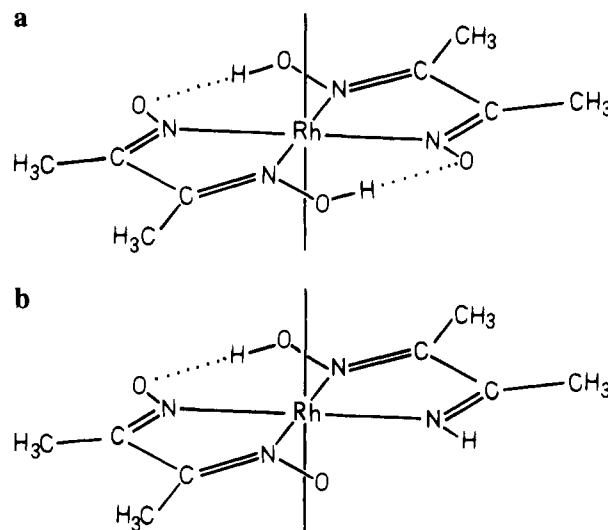


Figure 1. (a) $(\text{Hdmg})_2$ complexes. (b) $(\text{Hdmg})(\text{Hbdio})$ complexes.

lead to the reduction of one of the equatorial ligands: the base-catalyzed decomposition of methylcobaloxime produces methane and a hydroxo aquo cobaloxime derivative in which one oxime linkage has been hydrated to carbinolamine.⁶ The reduction-induced cleavage of the Co–C bond in $\text{Co}(\text{dmgBF}_2)_2(\text{A})\text{R}$ (A = pyridine or H_2O) results in the formation of an alkene and a Co(II) complex with reduced macrocycle.⁷

We previously described the synthesis of $\text{Rh}(\text{Hdmg})_2(\text{PChx}_3)\text{Cl}$ and $\text{Rh}(\text{Hdmg})_2(\text{PPR}^t_3)\text{Cl}$ by reduction of $\text{Rh}(\text{Hdmg})(\text{H}_2\text{dmg})(\text{Cl})_2$, addition of the phosphine, and reoxidation in the air.⁸

[†] Università di Trieste.

[‡] Università di Ancona.

[⊗] Abstract published in *Advance ACS Abstracts*, October 1, 1994.

- (1) Bresciani Pahor, N.; Forcolin, M.; Marzilli, L. G.; Randaccio, L.; Summers, M. F.; Toscano, P. J. *Coord. Chem. Rev.* **1985**, *63*, 1 and references therein.
- (2) Toscano, P. J.; Marzilli, L. G. *Prog. Inorg. Chem.* **1984**, *31*, 105 and references therein.
- (3) Le Hoang, M. D.; Robin, Y.; Devynck, J.; Bied-Charreton, C.; Gaudemer, A. J. *Organomet. Chem.* **1981**, *222*, 311.
- (4) Lavalley, D. K. *The Chemistry and Biochemistry of N-Substituted Porphyrins*; VCH Publishers: New York, 1987.
- (5) Daikh, B. E.; Finke, R. G. *J. Am. Chem. Soc.* **1991**, *113*, 4160.

(6) Brown, K. L. *J. Am. Chem. Soc.* **1979**, *101*, 6600.

(7) Shi, S.; Bakac, A.; Espenson, J. H. *Inorg. Chem.* **1991**, *30*, 3410.

Here we report the synthesis, X-ray structural characterization, and spectral and electrochemical properties of some Rh(III) complexes of the new equatorial moiety (Hdmg)(Hbdio) (Hbdio = 2,3-butanedione 2-imine 3-oximate) obtained by following the procedure mentioned above⁸ using PEt₃ and PBuⁿ₃. With these good donor and small cone angle phosphines, the reaction causes the reduction of one of the four equatorial oximes to imine (Figure 1b).

Experimental Section

Synthesis. [Rh(Hdmg)(Hbdio)(PR₃)₂]⁺ClO₄⁻·H₂O (R = Et, Buⁿ). Rh(Hdmg)(H₂dmg)(Cl)₂ (0.405 g, 1 mmol) was suspended in 100 mL of methanol, and a solution of NaOH (0.2 g, 5 mmol) in water (5 mL) was added. The yellow solution so obtained was degassed, and under nitrogen atmosphere, 0.04 g (1 mmol) of NaBH₄ dissolved in water was added. The solution became black; it turned orange, under nitrogen, after the addition of phosphine (2 mmol), quickly for L = PEt₃ and more slowly for L = PBuⁿ₃. The mixture was stirred for an additional 30 min after the change of color. It was then filtered, and the filtrate was acidified (pH 6) with 1M HClO₄. An excess of NaClO₄ was added, and the solution was allowed to stand. The yellow crystals of the complex so obtained were recrystallized from methanol–water. Anal. Calcd for [Rh(Hdmg)(Hbdio)(PEt₃)₂]⁺ClO₄⁻·H₂O: C, 35.8; H, 6.9; N, 8.5. Found: C, 35.7; H, 6.9; N, 8.15. Calcd for [Rh(Hdmg)(Hbdio)(PBuⁿ₃)₂]⁺ClO₄⁻·H₂O: C, 45.8; H, 8.4; N, 6.7. Found: C, 44.6; H, 8.1; N, 6.2.

Alternatively, the reduction of the dichloro complex could be performed in the absence of NaBH₄ by addition of a strong excess of NaOH to a suspension of Rh(Hdmg)(H₂dmg)(Cl)₂ in ethanol, as previously described.⁹

Caution! Perchlorate salts are explosive and should be handled with great care. Quantities in excess of 30–40 mg should not be isolated; vacuum desiccation to extreme dryness should be avoided. Samples should always be looked upon as potential sources of ignition with respect to flammable organics.

[Rh(Hdmg)(Hbdio)(PR₃)₂]⁺[Rh(Hdmg)₂(Cl)₂]⁻·H₂O (R = Et, Buⁿ). The dichloro complex was dissolved in alkaline methanol and reduced with NaBH₄ as described above. An equimolar amount of phosphine was added, and the solution was stirred under nitrogen. After about 30 min, the solution was filtered, and the filtrate was acidified (pH about 6) with 1M HClO₄. The solvent was evaporated slowly, and the yellow crystals of the complex were collected. Anal. Calcd for [Rh(Hdmg)(Hbdio)(PEt₃)₂]⁺[Rh(Hdmg)₂(Cl)₂]⁻·H₂O: C, 34.5; H, 6.2; N, 11.5. Found: C, 34.8; H, 6.2; N, 11.6. Calcd for [Rh(Hdmg)(Hbdio)(PBuⁿ₃)₂]⁺[Rh(Hdmg)₂(Cl)₂]⁻·H₂O: C, 42.0; H, 7.4; N, 9.8. Found: C, 42.3; H, 7.4; N, 9.6.

Sometimes the NMR spectra showed the presence of the corresponding [Rh(Hdmg)₂(PR₃)₂]⁺ compounds, in just traces for PEt₃ and in significant amounts for PBuⁿ₃. With PPh₂Me, this route always led to about 1:1 mixtures of [Rh(Hdmg)(Hbdio)(PPh₂Me)₂]⁺ and [Rh(Hdmg)₂(PPh₂Me)₂]⁺; small amounts of Rh(Hdmg)₂(PPh₂Me)Cl were also detected.

Crystal Data. [Rh(Hdmg)(Hbdio)(PEt₃)₂]⁺[Rh(Hdmg)₂(Cl)₂]⁻·H₂O crystallizes as yellow prisms. Cell constants were obtained from least-squares refinement, using the setting angles of 25 reflections in the range 13 < θ < 18° measured by an Enraf-Nonius CAD4 single-crystal diffractometer equipped with a graphite crystal, incident-beam monochromator, and Mo Kα radiation. On the basis of the Niggli matrix, the choice of the triclinic unit cell was unambiguous. The crystal parameters and the basic information on data collections and structure refinements are summarized in Table 1.

Lorentz and polarization corrections were applied. An empirical absorption correction based on a series of ψ scans was applied; the relative transmission coefficients ranged from 0.868 to 0.999 with an average value of 0.936. A secondary extinction correction was applied.¹⁰ The final coefficient, refined in least-squares, was 4(1) × 10⁻⁸. Intensities of equivalent reflections were averaged.

Table 1. Crystallographic Data for [Rh(Hdmg)(Hbdio)(PEt₃)₂]⁺[Rh(Hdmg)₂(Cl)₂]⁻·H₂O

C ₂₈ H ₆₀ Cl ₂ Rh ₂ N ₈ O ₈ P ₂	fw 975.50
a = 8.181(3) Å	space group P $\bar{1}$ (No. 2)
b = 11.245(4) Å	T = 20 °C
c = 11.579(5) Å	λ = 0.710 69 Å
α = 92.16(2)°	ρ _{calc} = 1.54 g/cm ³
β = 94.47(2)°	μ = 10.3 cm ⁻¹
γ = 98.67(2)°	R(F _o) ^a = 0.033
V = 1048.5(7) Å ³	R _w (F _o) ^b = 0.032
Z = 1	

$$^a R = \frac{\sum(|F_o| - |F_c|)}{\sum|F_o|}. \quad ^b R_w = \frac{[\sum w(|F_o| - |F_c|)^2 / \sum w|F_o|^2]^{1/2}}{}$$

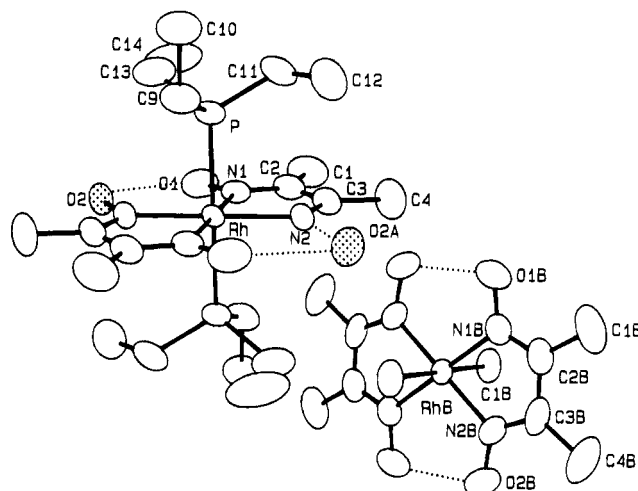


Figure 2. Electron density map in the coordination plane of the Rh(Hdmg)(Hbdio) equatorial moiety. The scheme of interpretation of the disorder is also depicted.

The analysis of the Patterson map suggested that two crystallographically independent Rh atoms should be located at the symmetry centers 0, 0, 0 and 0, 1/2, 1/2, in the P $\bar{1}$ space group. A typical electron density distribution on the equatorial coordination plane of the cation is depicted in Figure 2. These maps showed that the peak corresponding to the oxime O2 atom was split into two peaks of half-weight. Therefore, the two peaks were attributed to an oxime O2 atom and to a H₂O molecule (O2A) (see next section), both with half-occupancy, in agreement with the crystallographic symmetry which requires a statistical disorder of the equatorial moiety. The anisotropic refinement by full-matrix least-squares methods, including the constant contribution of H atoms, confirmed the half-occupancy of O2 and O2A, giving an R index of 0.033. The final difference Fourier map showed the higher peaks, with a maximum height of 0.81 e/Å³, located around the Rh atoms. The disorder of the structure led to some doubts about the choice between the centric and the acentric space group, which does not imply a statistically disordered equatorial moiety of the cation. The anisotropic refinement, in the space group P₁, reached convergence very slowly, although the final cycle gave an R index of 0.029. However, this minimization led to unreliable positional parameters. In fact, the chemical equivalent bond lengths, especially for the anion [Rh(Hdmg)₂(Cl)₂]⁻, were significantly different, up to 20 times their estimated standard deviations. For this reason the centrosymmetric space group was chosen despite the slightly higher R value.

The final atomic coordinates and B_{eq} values for all the non-hydrogen atoms are reported in Table 2, and the bond lengths are given in Table 3.

Scattering factors were taken from Cromer and Waber.¹¹ Anomalous dispersion effects were included in F_c;¹² the values for Kf' and Kf'' were those of Cromer.¹³

(8) Asaro, F.; Dreos Garlati, R.; Pellizer, G.; Tauzher, G. *Inorg. Chim. Acta* **1993**, *211*, 27.

(9) Miller, J. D.; Oliver, F. D. *J. Chem. Soc., Dalton Trans.* **1972**, 2469.

(10) Zachariasen, W. H. *Acta Crystallogr.* **1963**, *16*, 1139.

(11) Cromer, D. T.; Waber, J. T. *International Tables for X-Ray Crystallography*; The Kynoch Press: Birmingham, England, 1974; Vol. IV, Table 2.2B.

(12) Ibers, J. A.; Hamilton, W. C. *Acta Crystallogr.* **1964**, *17*, 781.

(13) Cromer, D. T. *International Tables for X-Ray Crystallography*; The Kynoch Press: Birmingham, England, 1974; Vol. IV, Table 2.3.1.

Table 2. Positional Parameters and Esd's for $[\text{Rh}(\text{Hdmg})(\text{Hbdio})(\text{PEt}_3)_2]^+[\text{Rh}(\text{Hdmg})_2(\text{Cl})_2]^- \cdot \text{H}_2\text{O}$

atom	x	y	z	B (Å ²) ^a
Rh	0.000	0.000	0.000	3.335(6)
P1	0.0357(1)	-0.20537(7)	0.01456(7)	4.23(2)
O1	-0.3368(3)	-0.0542(2)	0.0767(2)	6.12(6)
N1	-0.1792(3)	-0.0237(2)	0.1119(2)	4.40(5)
N2	0.1289(4)	0.0451(2)	0.1548(2)	4.77(6)
C1	-0.2495(7)	-0.0168(4)	0.3145(3)	9.2(1)
C2	-0.1300(6)	-0.0034(3)	0.2227(3)	6.00(9)
C3	0.0455(6)	0.0362(3)	0.2454(3)	6.4(1)
C4	0.1284(9)	0.0647(5)	0.3654(3)	10.1(2)
C9	0.1806(6)	-0.2483(3)	-0.0838(4)	6.58(9)
C10	0.2226(6)	-0.3739(4)	-0.0777(4)	7.8(1)
C11	0.0997(6)	-0.2525(3)	0.1552(3)	6.38(9)
C12	0.2763(6)	-0.2132(5)	0.1984(4)	8.5(1)
C13	-0.1559(7)	-0.3133(4)	-0.0380(5)	8.0(1)
C14	-0.2778(7)	-0.3326(5)	0.0409(7)	11.4(2)
RhB	0.000	0.500	0.500	3.599(6)
C11B	0.0992(1)	0.4486(1)	0.32437(7)	5.66(2)
O1B	0.1329(4)	0.2995(2)	0.6023(3)	6.82(7)
O2B	0.1741(4)	0.7438(2)	0.4964(3)	7.14(7)
N1B	0.1672(3)	0.4171(3)	0.5834(2)	4.86(6)
N2B	0.1877(4)	0.6330(3)	0.5306(2)	5.03(6)
C1B	0.4476(5)	0.4322(5)	0.6793(4)	8.2(1)
C2B	0.3078(4)	0.4809(4)	0.6162(3)	5.34(8)
C3B	0.3209(4)	0.6062(4)	0.5864(3)	5.56(8)
C4B	0.4728(6)	0.6989(5)	0.6153(5)	8.9(1)
O2A	0.4442(6)	0.0962(5)	0.1309(4)	6.0(1) ^b
O2	0.3169(5)	0.0817(4)	0.1573(4)	4.9(1) ^b

^a Anisotropically refined atoms are given in the form of the isotropic equivalent displacement parameter defined as $(4/3)[a^2B(1,1) + b^2B(2,2) + c^2B(3,3) + ab(\cos \gamma)B(1,2) + ac(\cos \beta)B(1,3) + bc(\cos \alpha)B(2,3)]$. ^b Atom with half-occupancy.

Table 3. Bond distances (Å) for $[\text{Rh}(\text{Hdmg})(\text{Hbdio})(\text{PEt}_3)_2]^+[\text{Rh}(\text{Hdmg})_2(\text{Cl})_2]^- \cdot \text{H}_2\text{O}$

Rh-P1	2.3817(8)	C9-C10	1.506(6)
Rh-N1	2.025(3)	C11-C12	1.487(6)
Rh-N2	2.015(2)	C13-C14	1.403(9)
P1-C9	1.810(5)	RhB-C11B	2.3320(9)
P1-C11	1.795(4)	RhB-N1B	1.980(3)
P1-C13	1.877(5)	RhB-N2B	1.976(3)
O1-N1	1.312(4)	O1B-N1B	1.340(4)
N1-C2	1.316(4)	O2B-N2B	1.339(4)
N2-C3	1.294(5)	N1B-C2B	1.282(4)
N2-O2	1.529(5)	N2B-C3B	1.304(5)
C1-C2	1.495(6)	C1B-C2B	1.494(6)
C2-C3	1.438(6)	C2B-C3B	1.453(6)
C3-C4	1.499(5)	C3B-C4B	1.504(6)

All calculations were performed on a VAX computer using the MolEN package.¹⁴

NMR Measurements. The NMR spectra were recorded on a Bruker WP80 spectrometer (¹H at 80 MHz, ¹³C at 20.1 MHz, ³¹P at 32.4 MHz) equipped with an ASPECT 2000 computer and on a JEOL EX-400 spectrometer (¹H at 400 MHz, ¹³C at 100.4 MHz, ³¹P at 161.7 MHz). For the ¹H and ¹³C spectra, TMS was used as internal standard in the CDCl₃ and (CD₃)₂CO solutions and DSS was used in the DMSO-*d*₆ solutions. For the ³¹P spectra, H₃PO₄ (10%) was used as external standard.

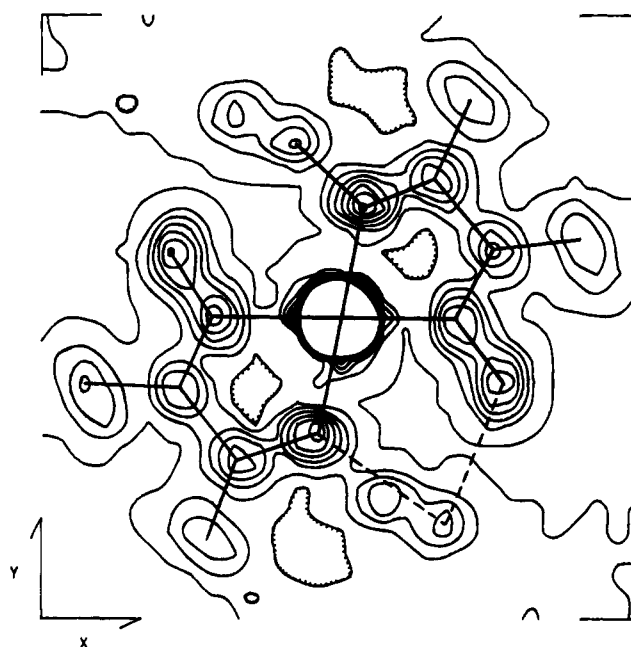
Variable-temperature ¹H and ¹³C spectra were recorded by using the JEOL NM-EVTS3 variable-temperature system.

Electrochemistry. Acetonitrile (AN) (Fluka) was dried over molecular sieves and stored under Ar. Dimethyl sulfoxide (DMSO) (Aldrich) was used as purchased without further purification. Tetraethylammonium perchlorate (TEAP) (Fluka) was recrystallized from water and vacuum-dried at 40 °C.

All the potentials were quoted against an aquo NaCl saturated calomel electrode (SCE) separated from the solution by a glass frit

Z = 0.00

1 Å

**Figure 3.** ORTEP drawing for the non-hydrogen atoms of the compound $[\text{Rh}(\text{Hdmg})(\text{Hbdio})(\text{PEt}_3)_2]^+[\text{Rh}(\text{Hdmg})_2(\text{Cl})_2]^- \cdot \text{H}_2\text{O}$. Dotted ellipsoids refer to the species O2 and O2A, with half-occupancy. For clarity, the counterparts of the latter atoms, referred by the crystallographic symmetry center on Rh, were omitted from the drawing.

filled with TEAP (0.1 M) in AN or DMSO solution. The complex concentration was about 10^{-3} M.

The working electrodes were a Smoler electrode¹⁵ for polarography and a Metrohm 663 stand for cyclic voltammetry (CV) on Hg drop (HMDE). The counter electrode was a Pt ring for CV or polarography and a Pt foil for controlled-potential reduction (CPR) separated from the bulk of the solution by a glass frit as was the reference electrode. The measurements were performed at 25 °C.

An Amel 568 function generator, a home-built potentiostat¹⁶ equipped with positive feedback, an Amel 863 recorder, and a Nicolet 4094C oscilloscope for fast signal recording were used. The data were transferred to an IBM 386 computer for handling.

Results and Discussion

Description of the Crystal Structure of $[\text{Rh}(\text{Hdmg})(\text{Hbdio})(\text{PEt}_3)_2]^+[\text{Rh}(\text{Hdmg})_2(\text{Cl})_2]^- \cdot \text{H}_2\text{O}$. The Fourier map analysis of the region of the cationic equatorial moiety was interpreted by assuming the presence of an imine group in the equatorial ligand and of a water molecule involved in hydrogen bonds with the adjacent oxime O1 and imine N2 atoms (Figure 2). Thus, the crystal is built up by $[\text{Rh}(\text{Hdmg})_2(\text{Cl})_2]^-$ anions, disordered $[\text{Rh}(\text{Hdmg})(\text{Hbdio})(\text{PEt}_3)_2]^+$ cations, and water molecules of crystallization in the ratio 1:1:1. The ORTEP drawing for the non-hydrogen atoms of the compound is shown in Figure 3. Dotted ellipsoids refer to the species O2 and O2A, with half-occupancy. For clarity the counterparts of the latter atoms, referred by the crystallographic symmetry center on Rh, were omitted from the drawing.

The analysis of the bond lengths shows that the Rh-N distances are slightly longer in the cation than in the anion (Table 3). The O2-N2 distance is particularly long, and this result should be ascribed to the difficulty in refining the very close species O2 and O2A with half-occupancy (1.099(7) Å). The statistical disorder of the equatorial moiety of the cation did

(14) MolEN, *An Interactive Structure Solution Procedure*; Enraf-Nonius: Delft, The Netherlands, 1990.

(15) Rossiter, B. W.; Hamilton, J. F. *Electrochemical Methods; Physical Methods of Chemistry*, Vol. II; Wiley: New York, 1986.

(16) Britz, D. *Electrochim. Acta* **1980**, 25, 1449.

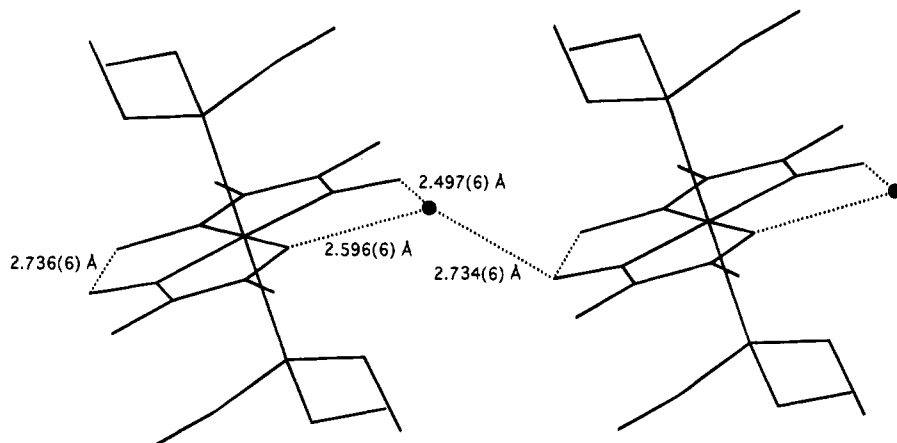


Figure 4. Inter- and intramolecular hydrogen-bonding scheme.

not allow any further comparison with the geometry of the anion, although the geometries of the Me–C–C–Me groupings appear very similar in the two ions (Table 3). The Rh–P and Rh–Cl distances are 2.3817(8) and 2.3320(9) Å, respectively, the latter being in the range (2.329–2.340 Å) reported for other complexes containing the $[\text{Rh}(\text{Hdmg})_2(\text{Cl})_2]^-$ anion.^{17,18} The difference of 0.059 Å between the Rh–P and Rh–Cl distances is close to that between the atomic radii of P (1.06 Å) and Cl (0.99 Å).

An interesting feature is that the cation binds one water molecule of crystallization (O2A) through two hydrogen bonds, one of 2.595(6) Å involving the imine N2 atom and the other of 2.496(6) Å involving the oxime O1 atom (Figure 4). Therefore the water molecule is strongly bonded to the cation. Pairs of cations, in the crystal, are bridged by the water molecules of crystallization, which, in addition to the above described H-bonds with one cation, makes a further H-bond with O1 of the other cation (Figure 4), at a distance of 2.734(6) Å.

As a trial to eliminate the statistical disorder in the cation, single crystals of $[\text{Rh}(\text{Hdmg})(\text{Hbdio})(\text{PEt}_3)_2]^+\text{ClO}_4^- \cdot \text{H}_2\text{O}$ were grown, but even in this compound the cation is located at a symmetry center. The crystals belong to the $P2_1/n$ space group, with $a = 11.968(3)$ Å, $b = 9.911(2)$ Å, $c = 13.529(3)$ Å, $\beta = 103.300(8)^\circ$, and $Z = 2$. The extended statistical disorder of the ClO_4^- anion and of the PEt_3 ligand did not allow the refinement of the crystal structure. However, the relative Fourier maps showed an electron density distribution very similar to that found for $[\text{Rh}(\text{Hdmg})(\text{Hbdio})(\text{PEt}_3)_2]^+[\text{Rh}(\text{Hdmg})_2(\text{Cl})_2]^- \cdot \text{H}_2\text{O}$.

NMR Spectra. In the $\{^1\text{H}\}^{31}\text{P}$ spectra of the $[\text{Rh}(\text{Hdmg})(\text{Hbdio})(\text{PR}_3)_2]^+$ species, the rhodium–phosphorus coupling constant, in the range 85–91 Hz for all the compounds, is similar to the one for $[\text{Rh}(\text{Hdmg})_2(\text{PPh}_3)_2]^+$ ⁸ and other rhodium(III) complexes containing two trans phosphines.¹⁹ The phosphorus is more deshielded in the $(\text{Hdmg})(\text{Hbdio})$ than in the corresponding $(\text{Hdmg})_2$ derivatives (Table 4).

In the ^1H spectra (Table 4) the methyls of $(\text{Hdmg})(\text{Hbdio})$ are responsible for four-well separated multiplets. Three of them are just triplets because of coupling with the two phosphorus atoms, while the highest frequency one is further split by coupling to the imine proton (Figure 5). The loss of symmetry in the electronic structure is also reflected in the $^5J(\text{P},\text{H})$ values, two of them (about 2 Hz) being larger and two (about 1 Hz)

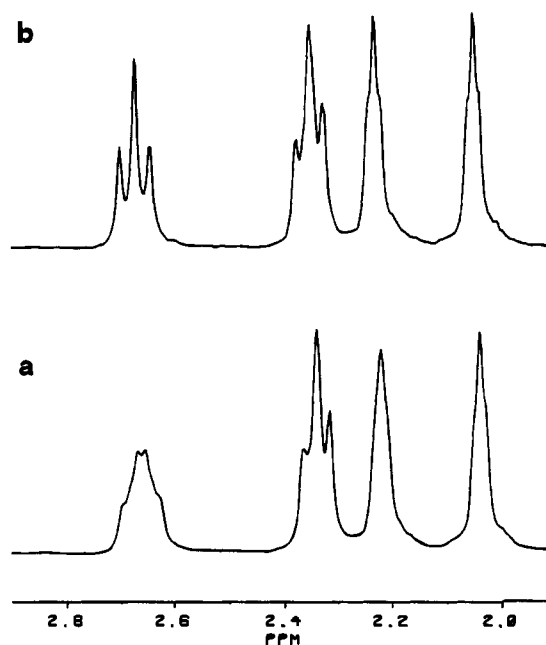


Figure 5. 80-MHz ^1H spectrum of $[\text{Rh}(\text{Hdmg})(\text{Hbdio})(\text{PEt}_3)_2]^+\text{ClO}_4^-$ in CDCl_3 . Equatorial methyls: (a) reference spectrum; (b) with decoupling of C=N–H at 10.76 ppm.

being smaller than those for the corresponding $(\text{Hdmg})_2$ derivatives (1.5 Hz). The imine proton frequency is not significantly influenced by temperature. For the $\text{Rh}(\text{Hdmg})_2$ and $\text{Rh}(\text{Hdmg})(\text{Hbdio})$ complexes, the protons of the O–H \cdots O bridges can be observed at low temperature (at room temperature they exchange fast with the water dissolved in the solvent). In CD_2Cl_2 at -70°C , the proton of the residual bridge for the $[\text{Rh}(\text{Hdmg})(\text{Hbdio})(\text{P}^i\text{Bu}_3)_2]^+$ complex resonates at 15.5 ppm; i.e., it seems that the removal of one O–H \cdots O bridge on going from $(\text{Hdmg})_2$ to $(\text{Hdmg})(\text{Hbdio})$ does not affect strongly the other one. In the $(\text{Hdmg})(\text{Hbdio})$ derivative with PPh_2Me , the equatorial methyls are about 0.8 ppm more shielded than those in the complexes with aliphatic phosphines. This has to be attributed to the magnetic anisotropy of the aromatic rings, as already reported for rhodoximes and cobaloximes.⁸ The phosphine protons give rise to complicated multiplets because of the various nuclear–nuclear couplings. It is noteworthy that in the $[\text{Rh}(\text{Hdmg})(\text{Hbdio})(\text{PPh}_2\text{Me})_2]^+$ derivative the phosphine methyl is a little more deshielded than that in the bis-(dimethylglyoximato) analogue.

^{13}C data are reported in Table 5. The lack of symmetry in the equatorial moiety affects strongly the $\{^1\text{H}\}^{13}\text{C}$ spectra where the three oxime carbons give rise to three resonances in the

(17) Simonov, Yu. A.; Nemchinova, L. A.; Ablov, A. V.; Zavadnik, V. E.; Bologa, O. A. *Zh. Strukt. Khim.* **1976**, *17*, 142.18

(18) Simonov, Yu. A.; Nemchinova, L. A.; Bologa, O. A.; *Kristallografiya* **1979**, *24*, 829.

(19) Grim, S. O.; Ference, R. A. *Inorg. Chim. Acta* **1970**, *4*, 277.

Table 4. ^{31}P and ^1H Data for $[\text{Rh}(\text{Hdmg})(\text{Hbdio})(\text{PR}_3)_2]^+\text{X}^-$ and $[\text{Rh}(\text{Hdmg})_2(\text{PR}_3)_2]^+\text{X}^-$ ^a

$[\text{Rh}(\text{Hdmg})(\text{Hbdio})(\text{PR}_3)_2]^+\text{X}^-$												
PR ₃	X	solvent	^{31}P	^1H							phosphine	
				(Hdmg)(Hbdio)					phosphine		Ar	CH ₃
				NH	CH ₃	CH ₃	CH ₃	CH ₃	CH ₃ ^b			
PPh ₂ Me	NO ₃	CDCl ₃	10.1 (91)	11.0	1.88 dt	1.17 (1.8)	1.37 (1)	1.24 (1)			7.70–7.20	2.25 vt
PPh ₂ Me	ClO ₄	CDCl ₃	9.62 (88)	11.52	1.78	1.18	1.40	1.28			7.65–7.3	2.14 vt
PEt ₃	ClO ₄	CDCl ₃	14.7 (88)	10.76	2.70 dt	2.37 (2)	2.25 (1)	2.10 (1)			CH ₂ 1.56	1.01 CH ₃
PEt ₃	Y	CDCl ₃	14.5 (88)	10.54	2.66	2.35	2.21	2.05	2.38		1.53	1.01
PEt ₃	Y	DMSO			2.52	2.32	2.14	1.96	2.19		1.52	0.93
PBu ⁿ ₃	Y	CDCl ₃		11.08	2.61	2.32	2.17	2.01	2.35		1.33 m	0.91 m
PBu ⁿ ₃	Y	DMSO	9.5 (88)									

$[\text{Rh}(\text{Hdmg})_2(\text{PR}_3)_2]^+\text{X}^-$												
PR ₃	X	solvent	^{31}P	^1H					phosphine			
				(Hdmg) ₂		phosphine			Ar	CH ₃		
				CH ₃	CH ₃	CH ₃	CH ₃	CH ₃				
PPh ₂ Me	ClO ₄	CDCl ₃	7.4 (88)	1.52 (1.5)					7.6–7.2			2.09 vt
PPh ₂ Me	ClO ₄	DMSO		1.46 (1.6)					7.67–7.37			2.09 vt
PBu ⁿ ₃	ClO ₄	CDCl ₃	8.9 (85)	2.34								

^a δ values in ppm; $|J|$ values in Hz in parentheses, first column $J(\text{Rh},\text{P})$, other columns $J(\text{H},\text{P})$. Y = $[\text{Rh}(\text{Hdmg})_2\text{Cl}_2]^-$. ^b In Y.

Table 5. ^{13}C Data for $[\text{Rh}(\text{Hdmg})(\text{Hbdio})(\text{PR}_3)_2]^+\text{X}^-$ and $[\text{Rh}(\text{Hdmg})_2(\text{PR}_3)_2]^+\text{X}^-$ ^a

$[\text{Rh}(\text{Hdmg})(\text{Hbdio})(\text{PR}_3)_2]^+\text{X}^-$																
PR ₃	X	solvent	(Hdmg)(Hbdio)								phosphine					
			C=N	C=N	C=N	C=N	CH ₃ CNH	CH ₃	CH ₃	CH ₃	CH ₃	ipso	ortho	meta	para	
PPh ₂ Me	NO ₃	CDCl ₃	178.2	155.9	153.7	147.3	21.5	12.0	11.6	11.4	6.6	126.1 125.6	131.4	128.9	131.5	
PPh ₂ Me	ClO ₄	CDCl ₃	178.3		153.8		22.0	12.4	11.9		7.1					
PPh ₂ Me	ClO ₄	DMSO	179.5	157.6	155.2	146.7	22.6	13.0	12.8	12.8	7.6	128.2 127.8	132.7	130.2	133.2	
PEt ₃	ClO ₄	CDCl ₃	179.1	156.7	154.2	146.6	23.2	13.2	12.4	11.8	12.2	7.1				
PEt ₃	Y	DMSO	180.0	158.6	155.5	146.6	22.9	14.2	13.3	13.0	12.9	8.1				
PBu ⁿ ₃	Y	CDCl ₃	178.8	156.4	153.7	145.5	20.2	12.6	12.2	11.7	19.6	24.6	24.6	24.6	13.5	
PBu ⁿ ₃	Y	DMSO	179.6	158.5	155.4	146.4	22.9	14.1	13.6	12.8	20.3	25.5	25.5	14.8		

$[\text{Rh}(\text{Hdmg})_2(\text{PR}_3)_2]^+\text{X}^-$																
PR ₃	X	solvent	(Hdmg) ₂				phosphine									
			C=N	CH ₃	CH ₃	ipso	ortho	meta	para							
PPh ₂ Me	ClO ₄	CDCl ₃	152.7	11.9		6.5										
PPh ₂ Me	ClO ₄	DMSO	153.8	13.1		7.3		126.2		132.9		130.4		133.2		
PBu ⁿ ₃	Y	CDCl ₃						19.3								
PBu ⁿ ₃	Y	DMSO						19.8								

^a δ values in ppm. Y = $[\text{Rh}(\text{Hdmg})_2\text{Cl}_2]^-$. The $[\text{Rh}(\text{Hdmg})_2\text{Cl}_2]^-$ C=N and CH₃ carbons resonate respectively at 152.6 and 12.3 ppm in CDCl₃ and at 150.1 and 13.2 ppm in DMSO. The $[\text{Rh}(\text{Hdmg})(\text{H}_2\text{dmg})\text{Cl}_2]$ carbons resonate respectively at 156.9 and 14.6 ppm in DMSO.⁸

range of rhodium^{20–22} and cobalt²³ bis(dimethylglyoximates) and the imine carbon resonates in the range 178–180 ppm, near

the imine carbons of the Co^{III}(DO)(DOH)pn complexes,²⁴ whose equatorial environment is a bis(dimethylglyoximate) moiety with an O–H···O bridge substituted by a $-(\text{CH}_2)_3-$ one. The corresponding equatorial methyl is considerably deshielded with respect to the other three, as well. The phosphine carbons are the X parts of AA'MX spin systems. As reported above for phosphorus atoms and protons, also the α -carbons of the axial

- (20) Randaccio, L.; Geremia, S.; Dreos Garlatti, R.; Tauzher, G.; Asaro, F.; Pellizer, G. *Inorg. Chim. Acta* **1992**, *194*, 1.
 (21) Bied-Charreton, C.; Gaudemer, A.; Chapman, C. A.; Dodd, D.; Das Gupta, B.; Johnson, M. D.; Lockman, B. L.; Septe, B. *J. Chem. Soc., Dalton Trans.* **1978**, 1807.
 (22) Giese, B.; Hartung, J.; Kesselheim, C.; Lindner, H. J.; Svoboda, I., *Chem. Ber.* **1993**, *126*, 1193.
 (23) Stewart, R. C.; Marzilli, L. G. *Inorg. Chem.* **1977**, *16*, 424.

- (24) Parker, W. O., Jr.; Zangrando, E.; Bresciani Pahor, N.; Marzilli, P. A.; Randaccio, L.; Marzilli, L. G. *Inorg. Chem.* **1988**, *27*, 2170.

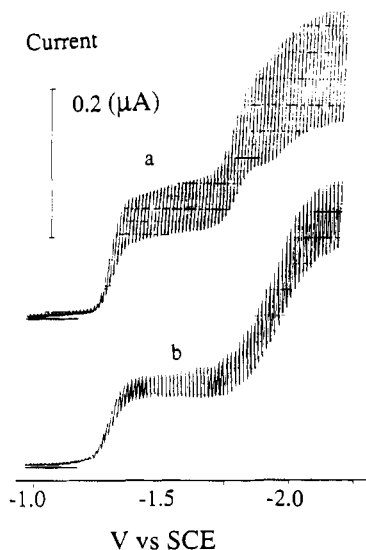


Figure 6. Polarography of the complex $[\text{Rh}(\text{Hdmg})(\text{Hbdio})-(\text{PEt}_3)_2]^+\text{ClO}_4^-$ at 5 mV/s (supporting electrolyte TEAP (0.1 M), $T = 25^\circ\text{C}$): (a) in AN, $E_{1/2}(\text{I}) = -1.332\text{ V}$, $E_{1/2}(\text{II}) = -1.80\text{ V}$, $E_{1/2}(\text{III}) = -2.05\text{ V}$; (b) in DMSO, $E_{1/2}(\text{I}) = -1.340\text{ V}$, $E_{1/2}(\text{II}) = -1.95\text{ V}$.

ligands are more deshielded in the (Hdmg)(Hbdio) than in the corresponding (Hdmg)₂ rhodium complexes. The asymmetry in the equatorial plane implies that the PPh₂Me phenyls in $[\text{Rh}(\text{Hdmg})(\text{Hbdio})(\text{PPh}_2\text{Me})_2]^+$ are diastereotopic, accounting for the presence of two multiplets for each kind of aromatic carbon. As expected, in the corresponding (Hdmg)₂ derivative, the phosphine phenyls are equivalent.

Electrochemistry of $[\text{Rh}^{\text{III}}(\text{Hdmg})(\text{Hbdio})(\text{PEt}_3)_2]^+\text{ClO}_4^-$

The polarographic behavior of the complex $[\text{Rh}^{\text{III}}(\text{Hdmg})(\text{Hbdio})(\text{PEt}_3)_2]^+\text{ClO}_4^-$ in AN solution is shown in Figure 6a. With concentrations ranging between 2×10^{-4} and 2×10^{-3} M, the first two waves are consistent with quasi-reversible one-electron processes; the third wave was not further investigated.

The CV in AN on HMDE showed three cathodic peaks with $E_{\text{pc}}(\text{I}) = -1.493\text{ V}$, $E_{\text{pc}}(\text{II}) = -2.128\text{ V}$, and $E_{\text{pc}}(\text{III}) = -2.300\text{ V}$ at 1 V/s. At this scan rate, there is no anodic peak to be assigned to the reoxidation of the products formed at the cathodic peaks. Both the first and second electron transfers are monoelectronic and diffusion controlled in the range from 0.1 to 100 V/s. At scan rates faster than 5 V/s the first cathodic peak shifted to $E_{\text{pc}} = -1.505\text{ V}$ and the corresponding anodic peak appeared at $E_{\text{pa}} = -1.448\text{ V}$. The ratio $i_{\text{pa}}/i_{\text{pc}}$ increased with the scan rate (Figure 7), showing that the electron transfer was followed by a relatively fast chemical reaction. The second cathodic peak showed no anodic counterpart up to 150 V/s. Repeated cyclic voltammetric scans showed that the electrode process starting at -2.15 V (second cathodic peak) causes the decrease of the peak current of the first cathodic process (Figure 8) and that the extent of the decrease is inversely proportional to the scan rate. If the CV scan was started from -2.300 V toward more positive potentials, no signals corresponding to the reductive process Rh(III)/Rh(II) were observed. Both results show that the product of the second electrode process reacts with the starting Rh(III) complex.

The polarography in DMSO (Figure 6b) showed a first wave, monoelectronic and electrochemically reversible, and a second wave, higher and corresponding to an electrocatalytic process.

As in AN, the CV in DMSO showed three cathodic peaks at -1.375 , -2.048 , and -2.250 V at 1 V/s. The anodic peak corresponding to the first cathodic peak appeared only at scanning rates higher than 15 V/s and was assigned to the reoxidation of Rh(II) species, confirming that a chemical reaction, faster in

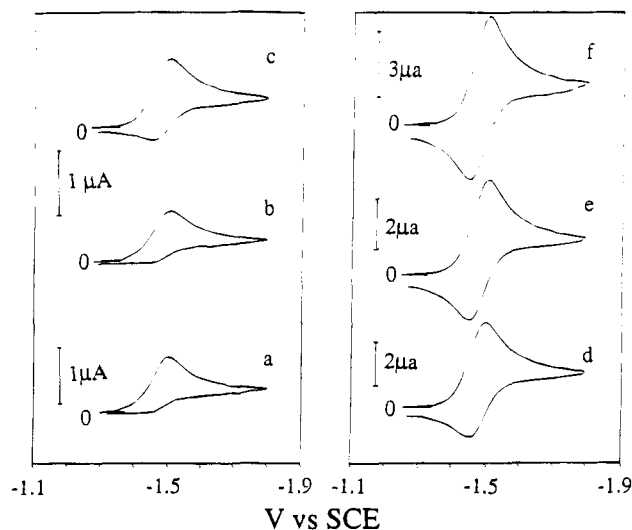


Figure 7. Cyclic voltammetry of the complex $[\text{Rh}(\text{Hdmg})(\text{Hbdio})-(\text{PEt}_3)_2]^+\text{ClO}_4^-$ in AN on an HMDE at the following scan rates: (a) 2 V/s; (b) 5 V/s; (c) 20 V/s; (d) 50 V/s; (e) 100 V/s; (f) 150 V/s.

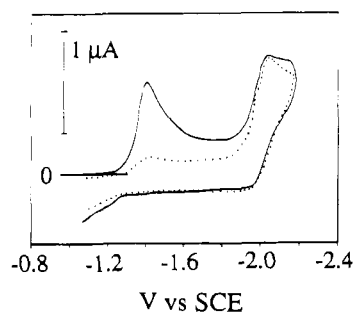


Figure 8. Cyclic voltammetry of the complex $[\text{Rh}(\text{Hdmg})(\text{Hbdio})-(\text{PEt}_3)_2]^+\text{ClO}_4^-$ in AN at a scan rate of 1 V/s on an HMDE. The solid line refers to the first scan; the dotted line, to the second scan.

DMSO than in AN, follows the electron transfer. The separation $E_{\text{pc}} - E_{\text{pa}}$ was 60 mV. The second cathodic peak had no anodic counterpart up to a scanning rate of 150 V/s. Repeated scanning between -1.0 and -2.1 V indicated that also in DMSO the product of the second electron transfer reacts with the starting Rh(III) complex.

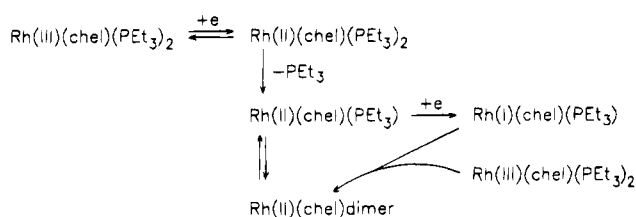
The CPR at $E = -1.400\text{ V}$, i.e. on the plateau of the first wave, showed that both in AN and in DMSO 1 faraday/mol of complex is required for the total disappearance of the wave. During the reduction in AN, a new oxidation wave ($E_{1/2} = -0.20\text{ V}$) appeared; it increased in proportion to the charge passed and was assigned to the oxidation of free PEt_3 . In DMSO, two oxidation waves (at -0.981 and -0.240 V) developed; the second one was assigned to free PEt_3 . The second cathodic wave of the starting Rh(III) complex was not affected by the CPR on the plateau of the first one. The CPR in DMSO, corresponding to the second polarographic wave (-2.1 V), revealed a catalytic electrode process.

Scheme 1 is the simplest mechanism consistent with the experimental results.

Both in AN and in DMSO the first electron transfer gives rise to a Rh(II) species, which releases the phosphine in a subsequent reaction, known to be the rate-determining step. The relationship between the $i_{\text{pc}}/i_{\text{pa}}$ ratio for the first couple of CV peaks and increasing scan rates (Figure 7) allowed us to estimate k values of 100 s^{-1} in AN and 600 s^{-1} in DMSO.²⁵ Both rates are much lower than expected²⁶ for the direct dimerization of a Rh(II) complex and are influenced by the solvent. The well-

(25) Nicholson, R. S.; Shain, I. *Anal. Chem.* **1964**, *36*, 706.

Scheme 1



(chel) = (Hdmg)(Hbdio)

known tendency of Rh(II) complexes to dimerize²⁷ and the appearance of an absorption at 450 nm, typical of Rh^{II}(Hdmg)₂ dimers,^{8,28} during the CPR at -1.400 V, suggest that the product of this reaction sequence is also a Rh(II)-Rh(II) dimer.

At more negative potentials in AN, a second monoelectronic electrode process gives rise to a Rh(I) derivative, which reacts rapidly with the starting Rh(III) complex; it is likely that the final product is still a Rh(II) dimer. In DMSO, a catalytic electrode process occurs that corresponds to the second polarographic wave and the second CV peak, implying a parallel oxidation of the Rh(I) complex with the solvent, also regenerating the Rh(II) species.

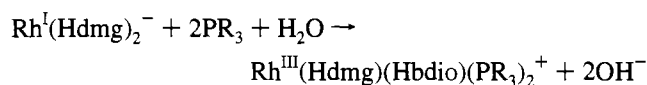
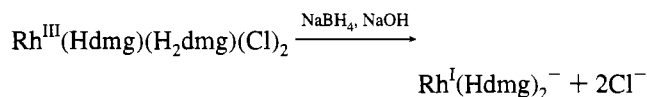
Comments on the Reactions between Rh(I) Rhodoxime and Phosphines. The reactions of Rh(I) rhodoxime with phosphines follow different routes depending on the properties of the phosphines. With PPrⁱ₃ and PChx₃, Rh(Hdmg)₂(PR₃)Cl derivatives are formed;⁸ with PEt₃ and PBuⁿ₃, the reduction of one of the equatorial oximes to imine occurs and the products are [Rh(Hdmg)(Hbdio)(PR₃)₂]⁺ complexes.

Inspection of the trend in the Σχ and the Tolman's cone angle values, which reflect respectively the electronic and the steric properties of the phosphines,²⁹ shows that the steric bulk of the phosphine is the main factor in determining whether the reaction products contain one or two phosphines. Only rhodoximes containing one phosphine are obtained when the steric bulk of the latter is large as for PPrⁱ₃ or PChx₃.

The reduction of the oxime group to imine occurs with phosphines of small size and good donor ability. The Rh^{III}-(Hdmg)(Hbdio) complexes are always found to contain two molecules of phosphine even if the latter is added in a 1:1 ratio with the dichloro complex, suggesting that the reduction of the equatorial moiety occurs after the entry of the second phosphine as a consequence of the high electron density on the metal. It is noteworthy that, during the synthesis of Rh(Hdmg)₂(PPrⁱ₃)Cl and Rh(Hdmg)₂(PChx₃)Cl, the addition of phosphine does not change the typical black color of the methanolic solution

of the Rh(I) complex and the corresponding Rh(III) complex is obtained only after oxidation in the air.⁸ Instead, after the addition of a 2-fold amount of PEt₃ or PBuⁿ₃, the solution turns orange under nitrogen, indicating that in this case the oxidation of Rh(I) does not involve O₂. The concurrence of this oxidation and of the formation of the species with a reduced oxime suggests that the redox reaction involves the metal ion and the equatorial moiety. Electron transfers between metal ions and macrocyclic equatorial ligands have been previously reported for Co(I) complexes with high delocalization in the equatorial plane.³⁰⁻³²

A possible reaction scheme is



The assumption that the loss of oxygen gives OH⁻ was made tentatively; further studies are in progress to verify it.

The (Hdmg)(Hbdio) moiety can be considered the product of a template synthesis leading to the deoxygenation of an oxime group of the bis(dimethylglyoximate) moiety under peculiar conditions, i.e. in the presence of a Rh(I) complex and phosphines of small size and good donor ability. The reduction appears to be very selective, as no evidence was found for the formation of compounds containing more than one imine group. Imine derivatives have sometimes been postulated as intermediates in the reductive cleavage of the N-O bond of the oximes by low-valent transition metal compounds,³³ but they could be isolated in only a few cases, for sterically protected groups; generally they hydrolyze to carbonyl derivatives. The high electron density on Rh(I) likely promotes, at least in the present case, the reduction of the oxime, and the coordination to Rh(III) enhances the stability of the imine toward hydrolysis.

Acknowledgment. We gratefully thank the MURST for financial support.

Supplementary Material Available: Tables of complete crystal data, hydrogen atom coordinates and isotropic thermal parameters, anisotropic thermal parameters for non-hydrogen atoms, and bond angles (3 pages). Ordering information is given on any current masthead page. Structure factors for the refinement in the *P* $\bar{1}$ space group and the positional parameters, bond lengths, and bond angles for the refinement in the *P*1 space group (17 pages) are available from the authors on request.

(26) Tinner, U.; Espenson, J. H. *J. Am. Chem. Soc.* **1981**, *103*, 2120.

(27) Jardine, F. H.; Sheridan, P. S. In *Comprehensive Coordination Chemistry*; Wilkinson, G., Gillard, R. D., McCleverty, J. A., Eds.; Pergamon Press: Oxford, U.K., 1987; Vol. 4.

(28) Caulton, K. G.; Cotton, F. A. *J. Am. Chem. Soc.* **1971**, *93*, 1914.

(29) Tolman, C. A. *Chem. Rev.* **1977**, *77*, 313.

(30) Walder, L.; Rytz, G.; Vögeli, U.; Scheffold, R. *Helv. Chim. Acta* **1984**, *67*, 1801.

(31) Takvoryan, N.; Farmery, K.; Katovic, V.; Lovecchio, F. K.; Gore, E. S.; Anderson, L. B.; Busch, D. *J. Am. Chem. Soc.* **1974**, *96*, 731.

(32) Hush, N. S.; Woolsey, I. S. *J. Am. Chem. Soc.* **1972**, *94*, 4107.

(33) Gilchrist, T. In *Comprehensive Organic Synthesis*; Trost, B., Fleming, I., Eds.; Pergamon Press: Oxford, U.K., 1991; Vol. 8, p 392.